

MODELLING OF THE ENCAPSULATION FACTORS FOR PHOTOVOLTAIC MODULES

P. Grunow¹ and S. Krauter²

¹Q-Cells AG, Guardianstr. 16, D-06766 Thalheim, Germany, E-mail: grunow@q-cells.com

²TU Berlin, Sec. EM 4, Einsteinufer 11, D-10587 Berlin, Germany, E-Mail: info@stefankrauter.com

ABSTRACT: The actual silicon crisis in photovoltaic industry forces the whole value chain to realize more installed W_p photovoltaic power out of every kg Silicon. This is approached through thinner wafers by the wafer producers, higher cell efficiencies by the cell manufacturers, and efficiency enhancements via improved encapsulation schemes at module production. Recently, some alternative encapsulation materials came in consideration, e.g. EVA replacements and cover glass with anti-reflective coatings. Cell technologies are changing as well. Some innovations are already adopted in standard products, but need to be tuned to each other. While the number of parameters involved has increased, it became cumbersome to minimize the optical losses experimentally. Modelling and variation of those parameters is performed to understand their interdependence and to propose optimal parameters sets, which can be used as good starting parameters for experimental probing.

Keywords: anti-reflective coating, modules, optical losses

INTRODUCTION

In this paper a simple algorithm for modelling the optical losses of encapsulated solar cells is developed. The anti-reflective coating (ARC) of the cell, i.e. silicon nitride (SiN_x) single layer, as the actual standard, plays a key role in the encapsulation behaviour. The optical losses in the module after encapsulation are highlighted in detail by calculating the reflectance and absorption of the different layers with the given optical constants of silicon [1] silicon nitride [2], ethylene vinyl acetate EVA [3] and solar glass [4]. Finally, the model is used to demonstrate the limits of the state-of-the art encapsulation technology on next generation silicon cells with improved spectral response (SR).

THEORETICAL APPROACH

EQE of the encapsulated cell

The short circuit current of the encapsulated cell in the module is calculated from the measured external quantum efficiency (EQE) of the cell in air. Together with the cell's reflectance spectrum (either measured or calculated from n_{SiN_x} and d_{SiN_x}) and the calculated losses due to the absorption and reflectance of the module encapsulation, see Fig. 1, the EQE of the module is:

$$EQE_{\text{module}} = EQE_{\text{cell/air}} \frac{(1 - A_{\text{SiN}_x})}{(1 - A_{\text{SiN}_x})} \cdot (1 - A_{\text{Encaps}}) \cdot \dots \quad (1)$$

$$\dots \frac{(1 - R_{\text{glass/air}})(1 - R_{\text{glass/EVA}})(1 - R_{\text{cell/EVA}})(1 + (1 - A_{\text{Encaps}})^2 R_{\text{glass/air}})}{(1 - R_{\text{cell/air}})}$$

The last factor in the numerator is describing the effect of multiple reflections, where higher orders with more than two reflections hitting the surface of the cell are neglected. The reflection at the EVA/glass interface is omitted for the multiple reflections as well, because $R_{\text{glass/EVA}}$ is below 0.1% for the sensitive range of silicon

cells between 300 nm to 1200 nm.

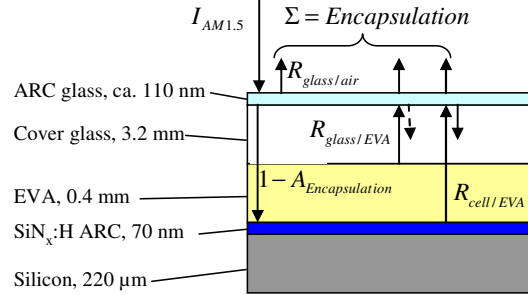


Fig. 1. Reflectance and absorption losses after encapsulation of a solar cell.

A_{SiN_x} and $A_{\text{SiN}_x'}$ serve to differentiate between alternative silicon nitride layers with different parameters. The reflectance and absorption of the different layers are calculated in detail in the next section. The short circuit photocurrent of the encapsulated cell in the module calculates to:

$$I_{SC,\text{module}} = \int_{300\text{ nm}}^{1200\text{ nm}} \frac{q\lambda}{hc} \cdot EQE_{\text{module}} \cdot I_{AM1.5} \cdot d\lambda \quad (2)$$

with $I_{AM1.5}(\lambda)$ as the global solar spectrum in steps of 10 nm taken from IEC 60904-3 Ed. 2 [5].

Reflectance

The reflectance of the SiN_x coated cell $R_{\text{cells/air}}$ in air or $R_{\text{cell/EVA}}$ in EVA is given by [6]:

$$R_{\text{cell}} = \frac{|\tilde{n}_0 m_{11} + \tilde{n}_0 \tilde{n}_{\text{Si}} m_{12} - m_{21} - \tilde{n}_{\text{Si}} m_{22}|^2}{|\tilde{n}_0 m_{11} + \tilde{n}_0 \tilde{n}_{\text{Si}} m_{12} + m_{21} + \tilde{n}_{\text{Si}} m_{22}|^2} \quad (3a)$$

with the transfer matrix

$$\begin{pmatrix} m_{11} & m_{12} \\ m_{21} & m_{22} \end{pmatrix} = \begin{pmatrix} \cos \delta_{SiNx} & i \sin \delta_{SiNx} / \tilde{n}_{SiNx} \\ i \tilde{n}_{SiNx} \sin \delta_{SiNx} & \cos \delta_{SiNx} \end{pmatrix} \quad (3b)$$

where \tilde{n}_i are the complex refractive indices for the incident medium \tilde{n}_0 , i.e., air or EVA, respectively, for silicon \tilde{n}_{Si} and for the silicon nitride layer \tilde{n}_{SiNx} in the complex form:

$$\tilde{n}_i = n_i - i k_i \quad (3c)$$

and

$$\delta_{SiNx} = \frac{2\pi d}{\lambda} \tilde{n}_{SiNx} \quad (3d)$$

The above formulas were implemented in an Excel worksheet (enabled to operate with complex arguments by the Add-in "Technical analysis functions"). The reflectance on the thick adjacent layers, e.g. glass/EVA, glass/air was calculated by:

$$R_{glass/EVA}(\lambda) = \frac{(n_{glass} - n_{EVA})^2 + k_{EVA}^2}{(n_{glass} + n_{EVA})^2 + k_{EVA}^2} \quad (4)$$

The reflectance of the encapsulation is not used for the modelling here, but might be the parameter accessible in the experiment. Taking multiple reflections into account, it is:

$$R_{Encapsulat} = R_{glass/Air} + R_{glass,EVA} + R_{cell/EVA} (1 - A_{Encaps})^2 (1 - R_{glass/air})^2 + \dots \\ \dots + \frac{R_{cell/EVA}^2 \cdot R_{glass/air} (1 - A_{Encaps})^4 (1 - R_{glass/air})^2}{1 + R_{cell/EVA} \cdot R_{glass/air} (1 - A_{Encaps})^2} \quad (5)$$

ARC glass

The reflectance $R_{glass/air}$ at the interface glass/air - with or without anti-reflective coating - was extracted

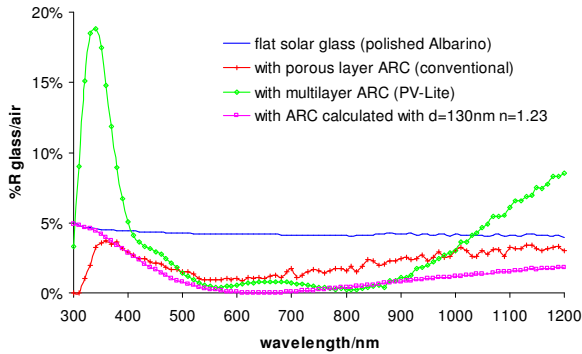


Fig. 2. Effect of different anti-reflective coatings on the reflectance of the glass/air interface

from measured glass reflectance and transmittance spectra provided by [4] and using Eq. 5 to separate the effect of the two different interfaces.

Recently, Wohlgemuth et al. [7] showed an increase of 2.4% in the power output at STC and an additional increase of 1.8% in the performance ratio using cover glasses with anti-reflective coating. The glass suppliers prospect a power increase of 2.7% to 3.1% at standard

test conditions (STC). We calculated an possible increase of 3.7% for a single layer ARC on a polished glass surface with a refractive index of $n=1.23$ and a thickness of 130 nm. As a design rule, one should optimise the encapsulated cell to uncoated glass first and then adjust the ARC to it, because the effects from the glass ARC are much smaller than those from the ARC of the cell. The multi-layer ARC in Fig. 2 might be an exception, because of its high reflectance beyond the anti-reflective window.

Absorption

The absorption A_{SiNx} of the $SiNx$, is given by $1 - \exp(-\alpha_{SiNx} d_{SiNx})$ with $\alpha_{SiNx} = 4\pi k_{SiNx} / \lambda$.

The absorption in EVA and glass is calculated using thicknesses of 0.4 mm and 3.2 mm, respectively, which are well established values in industrial practice regarding module reliability. The optical constants for EVA and glass are taken from [3],[4].

$$1 - A_{Encaps} = \exp(-\alpha_{EVA} d_{EVA}) \cdot \exp(-\alpha_{glass} d_{glass}) \quad (6)$$

The module's "zero-depth concentrator"-effect resulting from the backscattering of the incident light at the white back sheet material (Tedlar®) from the spacings between the cells in the module were determined experimentally to 0.4% additional I_{sc} current per 1 mm spacing for 156 mm cells in the range of 3-5 mm cell spacing. This is in good agreement with the calculated value of 1.3% for 3 mm spacings as provided by McIntosh et al. [8].

The reflections of the soldered interconnectors covering typically 3% of the cell area add only 0.13%. Both effects sum up to 1.4% in total for 3 mm 156 mm square cells.

Texturization

The effect of the texturization of the cell's surface is approximated by assuming a second impact of the light reflected at the textured surface, i.e. $R_{cell/air}$ is replaced by $R_{cell/air}^2$.

This approximation is already a good guess to describe the difference in the experimental EQE between the nearly flat, alkaline etched, multi crystalline cell in Fig. 3 and the alkaline textured mono crystalline cell as measured by Fraunhofer ISE Freiburg. The shading loss from the metal front grid is 8% for both cells.

An "improved cell" was modelled in Fig. 3 by setting the quantum efficiency to be constant in the wavelength range starting from 550 nm to sketch the effect of an ideal emitter, what increases the I_{sc} by +1.6%. In the infrared region the collection efficiency was fixed for values of $\lambda > 700$ nm and the decrease of the silicon absorption was replaced by the effect of an Lambertian back reflector on the back of the cell, which can be described with a path length enhancement of $4n_{Si}^2$ [9] or +10% in I_{sc} in the present case or a total of 40 mA/cm².

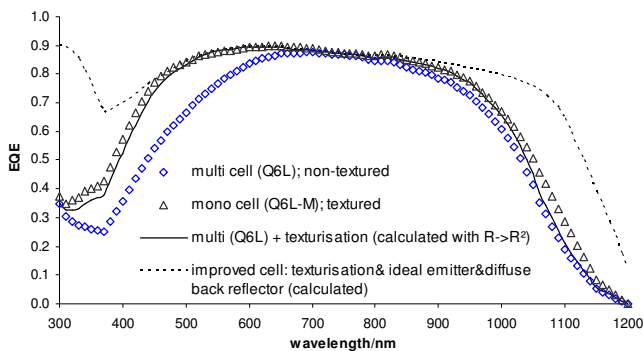


Fig. 3. Measured and calculated EQE as used in the calculation of the encapsulation effects

RESULTS

SiN_x layer optimization

Fig. 4 shows the variation of the short circuit current for an encapsulated multi cell (Q6L) as a function of the refractive index and thickness of the SiN_x layer.

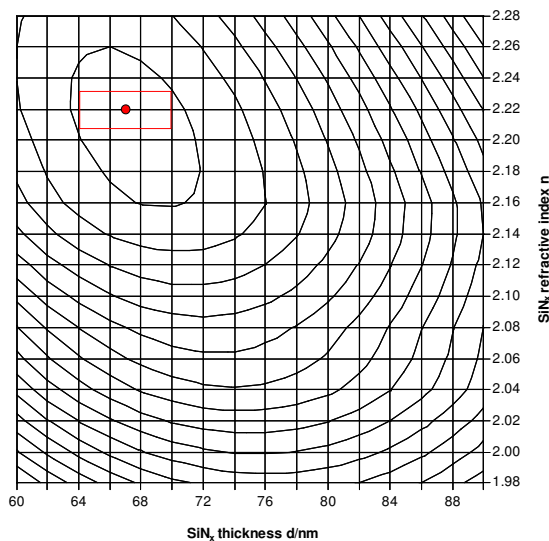


Fig. 4. Change of the I_{sc} of an encapsulated multicrystalline cell (Q6L) in steps of 0.2%. Typical process tolerances for the thickness are $d \pm 3$ nm and $n \pm 0.01$ for the refractive index as indicated by the red rectangular.

The optimum value of $n_{SiN_x} = 2.22$ at 632.8 nm and $d = 67$ nm in Fig. 4 confirm the results found by Doshi [10] and Ekai [11]. An independent set of cells with a total I_{sc} variation of 6% as a result from differences in the wafer quality, i.e. variations in the infrared region of the spectral response (SR) resulted in a deviation of ± 0.01 for the found optimal refractive index and ± 1 nm for the found thickness. While Doshi found a refractive index of

$n = 2.23$ and $d = 68$ nm for the encapsulated cell, Ekai et al. [11] calculated $n = 2.20$ and $d = 67$ nm for flat cells and $n = 2.10$ and $d = 70$ nm for V-grooved cell surfaces, respectively.

Taking the zero-depth concentrator effects into account (1.4% enhancement), the encapsulation gain for weakly or non-textured multi cells is 4.8% when using an ideal ARC glass and it is 1.1% without ARC glass.

Encapsulation factor

Fig. 5 shows the principal agreement between calculated and experimental data.

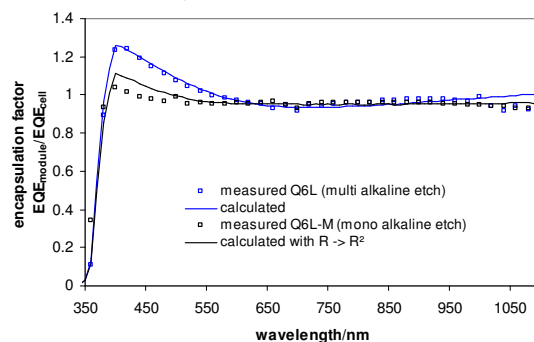


Fig. 5. Encapsulation effect for a multi-crystalline and a mono-crystalline cell as measured and calculated

A detailed analysis of the optical losses is plotted in Fig. 6 for a multi cell. The contribution of each loss mechanism was calculated by setting all other losses to zero. In consequence the total loss is slightly smaller than the direct sum of the single losses.

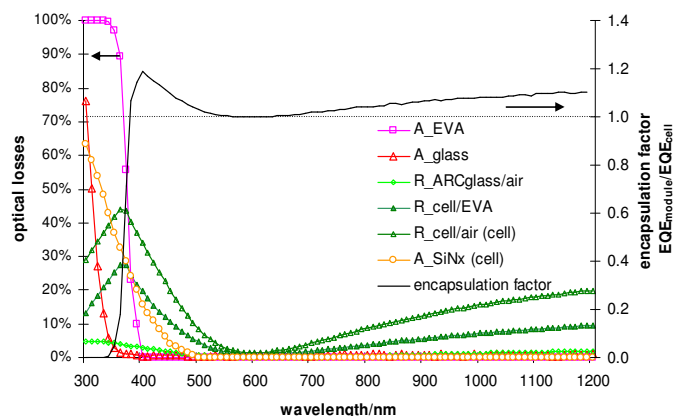


Fig. 6. Calculated losses and encapsulation factor.

The cell's reflectance is the major loss either in air as in the module. The encapsulated cell is gaining mainly in the range between 400 and 600 nm, where the index matching between silicon and EVA by the SiN_x layer results in reflection reductions of 50%.

Encapsulation of textured cells

Fig. 7 shows the difference in the cell reflectance in air and with EVA for the non-textured multi cell (0% textured area), an intermediate case with 50% textured area and the 100% textured cell (e.g. mono cells).

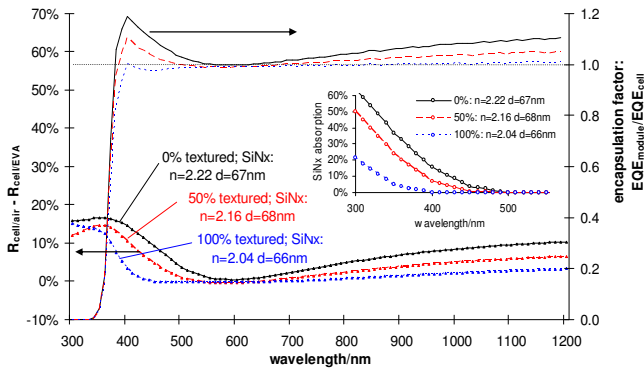


Fig. 7. Degree of texturization and its effect on the optical losses and the encapsulation factor

Fig. 7 demonstrates the decrease of the encapsulation gain with increasing degree of texturization. It decreases in steps of 2%.

After optimisation of the SiN_x parameters for each degree of texturization, see curve descriptions in Fig.7, the encapsulation gain decreases again, see Table 1, but the *I*_{sc} will increase overall, i.e. results in a better utilization of the given wafer material.

<i>I</i> _{sc} cell	real cell		improved cell (model)	
	31.1 mA/cm ²		37.8 mA/cm ²	
optimum SiN _x	n=2.22, d=67 nm		n=2.04, d=66 nm	
	air	module	air	module
SiN _x absorption (cell)	-1.3%	-1.3%	-0.2%	-0.2%
EVA absorption	-	-1.3%	-	-2.4%
glass absorption	-	-0.8%	-	-0.9%
ARCglass/air reflection	-	-0.7%	-	-0.8%
cell reflection	-9.6%	-4.8%	-2.1%	-0.9%
total	-10.5%	-7.5%	-2.2%	-4.3%
encapsulation gain		3.4%		-2.1%

Table 1: *I*_{sc} losses in air and in the module with a standard cell and the improved cell from Fig. 3 without considering the zero-depth concentrator effect

For the fully textured cells, the optimum for the SiN_x antireflective layer shifted to a lower refractive index of *n*= 2.04 and a slightly lower thickness of *d*= 66 nm, because it is more effective to reduce the SiN_x absorption through lowering *n* and *d*, while reduction of the cell reflectance is nearly obsolete for textured cells.

UV absorption in EVA has become the major loss mechanism for the improved cell in Table 1. The effect of the ideal emitter, i.e. 1.6% increase in the UV, is completely blocked by the EVA.

CONCLUSION

A simple model was developed to describe the complex system of an encapsulated solar cell, which can be implemented in spread-sheet program. The optimum parameters for the SiN_x layer of non-textured cells are *n*_{SiN_x}= 2.22 and *d*_{SiN_x}= 67nm. The zero-depth concentrator effect adds 1.4% in *I*_{sc} for 3 mm spaced 156 mm square cells on white Tedlar[®]. The total encapsulation gain sums up to 1.1%. With increasing degree of texturization the optimum refractive index of the SiN_x decreases. For fully textured cells (e.g. mono cells) it is *n*_{SiN_x}= 2.04. ARC cover glass does not need adjustments on the cell side and an ideal gain of 3.7% was calculated. The effect of shallower emitters is likely to be limited by the EVA absorption. Implications on the optical losses for non-STC conditions are considered in an accompanying paper [12].

ACKNOWLEDGEMENTS

We would like to thank Andreas Nositschka from Saint-Gobain Glass Germany for the optical data of solar glass, J-F. Lelièvre from the UMR-CNRS in Lyon for providing the optical constants of silicon nitride, V. Hoffmann and D. Binder from Q-Cells AG for data on the SR and on the concentration effect of encapsulated cells and K. McIntosh for calculating the latter effect for the modules considered in this paper.

REFERENCES

- [1] M.A. Green and M. Keevers *Prog in Photovoltaics*, Vol. 3, 1995, p. 189
- [2] Lelièvre et al, Conf. Record of the 31st IEEE PV Specialists Conference, 2005, p. 1111.
- [3] Nagel et al. *2nd WCPEC*, Vienna, 1998.
- [4] A. Nositschka, Saint-Gobain Glass Germany GmbH, private communication
- [5] IEC 82/347/CD Photovoltaic devices - Part 3.
- [6] O.S. Heavens, Dover Publications Inc. 1991.
- [7] J. Wohlgemuth et al. *IEEE*, 2005, p.1015.
- [8] K. R. McIntosh et al. *Prog. in Photovoltaics* **14**, 2006, p. 167
- [9] E. Yablonovitch, *J. Opt. Soc. Am.* **72** (1982) p. 899.
- [10] Doshi, P. et al. *IEEE Trans. Electron Devices* **44**, 1997, p. 1417
- [11] R. Ekai et al, *Proc. of the 2nd PV World Conference*, Vienna, 1998, p.1430.
- [12] S. Krauter, P. Grunow, *this conference*